Pure Appl. Geophys.

https://doi.org/10.1007/s00024-025-03688-0

Pure and Applied Geophysics

Can Contaminated Waters from the Fukushima Daiichi NPP Penetrate the East China Sea?

M. V. Budyansky,[1,2] M. Yu. Uleysky,[2] P. A. Fayman,[2] A. A. Didov,[1,2] M. A. Lebedeva,[1,2] A. A. Udalov,[2] T. V. Belonenko,[1] Danling Tang,[3] Xiaobo Yang,[3] and Sui Yi[4]

Abstract—Mesoscale eddies play a pivotal role in the dispersion and transport of pollutants in the ocean, influencing their horizontal and vertical distribution over vast areas. These rotating structures, ranging from tens to hundreds of kilometers in diameter, effectively trap, transport, and mix water masses, redistributing contaminants away from their sources. This study investigates the southward transport mechanisms of contaminated waters released from the Fukushima Daiichi Nuclear Power Plant (FDNPP), particularly near the Kuroshio Current. Using advanced Lagrangian modeling, we analyze the influence of mesoscale eddies, cross-jet transport, and interactions with adjacent water masses on the movement of pollutants into regions south of the Kuroshio. The findings reveal that the Kuroshio Current captures contaminated waters, forming cyclonic rings that detach and drive pollution southwestward. This process is further enhanced by the dissipation of cyclonic eddies, which facilitate the spread of contaminants toward the eastern periphery of the current. Cross-jet advection, resulting from the weakening of the Kuroshio near Taiwan, also contributes to westward transport. Additionally, the influence of East Asian monsoons introduces a 6-month recurrence cycle, sustaining long-term pollutant flux and promoting stable accumulation in the region. Three key mechanisms are identified for the successful transport of Lagrangian particles from FDNPP to the East China Sea: cross-jet transport in the Kuroshio Extension, leading to cyclonic ring formation, southwestward advection of these rings or their daughter eddies, and specific Kuroshio flow regimes allowing east-to-west pollutant transport.

Keywords: Lagrangian modeling, Fukushima Daiichi NPP, FDNPP, East China Sea, Kuroshio Current, Eddies, transport.

1. Introduction

By analogy with the Gulf Stream system, the current system located in the western half between 20° and 40° N, characterized by high flow velocity and positive water temperature anomalies, is called the Kuroshio System (Hiroaki, 2019; Takeyoshi et al., 2019; Belonenko et al., 2009). This system includes the Kuroshio proper, the Kuroshio Extension, and the northeastern branch of the Kuroshio, among others. The Kuroshio Current is part of the extensive anticyclonic gyre in the subtropical zone of the northern Pacific Ocean; it transports waters with high temperatures and salinity. The eastward flow, extending to 160° E, is called the Kuroshio Extension.

Contaminated waters discharged from the FDNPP following the 2011 accident have become a significant environmental issue, particularly for the marine ecosystems of the Pacific Ocean. The Kuroshio Current, one of the most powerful western boundary currents in the world's oceans, plays a pivotal role in the dispersion of this pollution. By transporting vast volumes of water from Japan's eastern coasts into the open Pacific, the current facilitates the movement of radioactive substances over long distances. Seasonal variations and interactions with other oceanic currents, such as the North Pacific Current, further allow pollutants to reach distant regions, including the coastal waters of North America and tropical areas. This underscores the complexity of monitoring and modeling pollution dispersion, as the movement of particles on such scales is influenced not only by the main current but also by mesoscale and submesoscale eddy structures, oceanic fronts, and vertical mixing processes.

[1] Saint Petersburg State University, Saint Petersburg 199034, Russia. E-mail: btvlisab@yandex.ru
[2] Il'ichev Pacific Oceanological Institute, Vladivostok 690041, Russia.
[3] Southern Marine Science and Engineering Guangdong Laboratory (Guangzhou), Guangzhou 511458, China.
[4] Institute for Ocean Engineering, Shenzhen International Graduate School, Tsinghua University, Shenzhen 518055, China.

Published online: 13 March 2025

In the literature, analyses of individual meanders and eddies of the Kuroshio Current are primarily based on temperature and current fields, as well as data from hydrodynamic modeling. Extensive scientific exploration of meanders and eddies in the interaction zone between the Kuroshio and Oyashio has resulted in numerous articles, the mere listing of which would span several pages. Here, we mention only those sources that provide a generalized overview. For example, the work of Kawai (1980) examines the formation, movement, and statistics of cold cyclonic eddies south of the Kuroshio. Kitano (1975, 1980) studies cyclonic eddies that emerge north of the Kuroshio, while Tomosada (1986) focuses on anticyclonic eddies. The authors note instances where an eddy ring drifts directly north or south of the Kuroshio, often merging with the current and later detaching from it again. These phenomena are also discussed in studies by Burkov (1992), Koshlyakov and Monin (1978), and Kamenkovich et al. (1986).

The structure of oceanographic fields south of the Kuroshio Extension is shaped by its meandering and the formation of numerous mesoscale eddies. It is well known that cyclonic eddies south of the Kuroshio Extension detach from the main jet but, through interaction with the surrounding environment, can merge back with the jet and subsequently detach again. The detachment of cyclonic rings from the Kuroshio jet is a complex physical process. Initially, the jet undergoes significant bending, drawing in subantarctic waters from the north into the curvature (potentially including waters contaminated by FDNPP). Gradually, the bend intensifies, and the two ends close, forming a ring. At the contact point between the boundary of the formed ring and the jet, a hyperbolic point emerges—a kind of "umbilical cord" connecting the nascent cyclonic ring to the jet (Prants et al., 2017c). The process by which waters from one side of the jet cross over to the other side is referred to as cross-jet transport (Prants et al., 2014, and references therein). The mechanism of meridional cross-jet transport involves the detachment of rings from the Kuroshio Extension. Such detachment of cyclonic rings containing FDNPP-contaminated water was previously examined by Prants et al. (2014).

Cyclonic eddies that detach from the jet initially move southward and then predominantly in westward and southwestward directions at speeds of approximately 3.8 cm/s (Aoki et al., 1995; Belonenko & Kubryakov, 2014; Bernstein & White, 1981; Li et al., 2024; Belonenko et al., 2024; Udalov et al., 2023). The periphery of such eddies consists of Kuroshio waters, while their cores are formed by northern waters, potentially including those contaminated by the FDNPP. As the eddies travel southward and southwestward, they gradually dissipate, releasing their transported waters, which then mix with the surrounding waters. The generation of warm anticyclonic eddies, as well as cold cyclonic eddies, is considered a dynamic consequence of the instability of jet currents in the Kuroshio interaction zone. Such eddies are referred to as frontal eddies because they form along fronts associated with jet currents. A combined form of eddy is also observed in the Kuroshio, where a fully developed eddy is located within a meander. Meander eddies sometimes detach from the jet and become independent eddies, while other times they decay without detaching or remerging with the current that generated them (Kamenkovich et al., 1986; Koshlyakov & Monin, 1978).

Burkov (1992), analyzing the results of the "Megapolygon" experiment, observed that some eddies contribute to meridional cross-jet transport in the Kuroshio Extension form when elongated intrusions of subarctic waters are disrupted by warm anticyclonic eddies (Delman et al., 2015). This interaction leads to the creation of isolated cyclonic eddies. Based on seasonal temperature maps over 10 years from 1955 to 1964, it was established that the number of cyclonic formations in the Kuroshio is higher during the colder half of the year (winter, spring) compared to the warmer half. Conversely, the number of anticyclonic eddies shows the opposite pattern. It was found that more cyclonic eddies form in spring and autumn, while more anticyclonic eddies form in summer and winter, corresponding to the seasonal peaks of Kuroshio transport. This finding aligns with the critical layer theory results of Ferrari and Nikurashin (2010) and Chen et al. (2014), which identified limited subsurface cross-Kuroshio Extension transport west of approximately 155° E, with increased meridional transport at this longitude.

Eddies, therefore, play a significant role in enhancing cross-frontal transport. Budyansky et al. (2015) demonstrated that anticyclonic Kuroshio warm core rings facilitated the transport of FDNPP-derived cesium, which was subducted and trapped in the subsurface core and intermediate water layers (100–500 m), northward of the subarctic front (Ueno et al., 2023). A detailed analysis of the Kuroshio field, including examples of the evolution of individual eddy structures, can be found in the works of Prants et al., (2014, 2017a, 2017b, 2017c), Budyansky et al. (2015), and Ueno et al. (2023).

Eddies play a critical role in the dispersion and transport of pollutants in the ocean. These rotating, mesoscale structures, which can range from tens to hundreds of kilometers in diameter, significantly influence the horizontal and vertical distribution of contaminants. Their importance lies in their ability to trap, transport, and mix water masses over vast distances, contributing to the redistribution of pollutants away from their original sources. The rotational motion of eddies creates convergence zones, which can trap pollutants within their cores, preventing their immediate dissipation into surrounding waters. This trapping mechanism can lead to localized areas of high contaminant concentration. Budyansky et al. () explored the potential for contaminated waters discharged from FDNPP to reach the coastal areas of the Kuril Islands, a region critical for Russian commercial fishing of fish and squid. These studies, along with works by Budyansky et al. (2015) and Prants (2014), Prants et al. (), highlighted the critical role of mesoscale eddies in spreading pollution across vast areas.

The primary objective of this study is to investigate and elucidate the mechanisms driving the southward transport of contaminated waters released from the FDNPP in the vicinity of the Kuroshio Current. This includes understanding how physical oceanographic processes, such as mesoscale eddies, cross-jet transport, and interactions with adjacent water masses, contribute to the spread of pollutants into regions south of the Kuroshio. To achieve this, the study employs advanced Lagrangian modeling techniques, which enable precise tracking of the trajectories of simulated particles representing pollution under the influence of the complex dynamics of ocean circulation.

2. Methods and Data

Lagrangian modeling is widely applied to investigate the transport characteristics of water masses (Budyansky et al., 2015; Prants et al., 2014, 2017a, 2017b). This approach provides precise insights into the movement and dispersion timeframes of water parcels by employing marker tracking techniques. These techniques involve simulating the trajectories of numerous passive tracers, which represent contaminants or other properties in the ocean. Lagrangian methods excel at simulating water circulation within oceanic basins, offering detailed analyses of transport and mixing by tracing the pathways of a large set of artificial passive particles.

In turbulent or chaotic flows, the visualization of particle trajectories, derived from satellite or numerical model velocity fields, often reveals a dense, intricate network of paths that can be challenging to decipher (Prants et al., 2017c). To apply this method, a dense grid of artificial particles is advected both forward and backward in time from a specific starting point. By analyzing the backward simulation, researchers can trace the origins of water masses reaching particular locations. The Lagrangian particle trajectories are calculated by numerically solving the 2D-advection equations:

$$\frac{d\lambda}{dt} = u(\lambda, \varphi, t), \ \frac{d\varphi}{dt} = v(\lambda, \varphi, t), \qquad (1)$$

where u and v are the angular zonal and meridional components of the GLORYS12V1 velocity field, respectively, and φ and λ are the latitude and longitude, respectively. Thus, we use two-dimensional currents from the GLORYS reanalysis to track the 2D movements of passive particles.

Angular velocities are utilized for their convenience in simplifying calculations involving the Earth's spherical geometry. To achieve high numerical precision, bicubic spatial interpolation is combined with temporal smoothing using third-order Lagrangian polynomials. The trajectories of

Lagrangian particles are determined by solving Eq. (1) through a fourth-order Runge–Kutta method, using a fixed time step of 0.001 days. This detailed numerical approach ensures both accuracy in simulations and reliability in the results.

In this study, stationary points in the velocity field for a specific date are identified on geographic maps using triangles and crosses. Triangles represent elliptic stationary points, which correspond to the centers of eddies where movement is stable and circular. Crosses denote hyperbolic stationary points, found between unstable eddies. At these points, water converges along two directions and diverges along two others, illustrating the dynamic interaction of flows (Budyansky et al., 2015; Prants et al., 2014, 2017a, 2017b, 2017c).

We utilize current velocities on the surface obtained from the global high-resolution ocean reanalysis GLORYS12V1 (Global Ocean Physics Reanalysis) with a spatial resolution of 1/12°, created using NEMO (Nucleus for European Modelling of the Ocean). The study covers one period from March 11, 2011, 3 years ahead in time. Essentially, we use a dataset from GLORYS12V1 spanning from March 11, 2011, to March 31, 2014.

The GLORYS12V1 product is based on a global real-time forecasting system. The GLORYS12V1 product is based on the NEMO model with forcing from the ECMWF ERA-Interim dataset. The GLORYS12V1 (NEMO) product assimilates in situ and satellite data from missions such as Topex/Poseidon, Jason-1, 2, MODIS Terra/Aqua, and AVHRR NOAA, as well as from drifting buoys such as Argo and drifters, other natural observations, and oceanographic surveys. Observations are assimilated into the NEMO model using a low-order Kalman filter. GLORYS12V1 accurately captures intricate surface dynamics at a small scale and shows robust agreement with independent data not included in the assimilation process. GLORYS12V1 offers a dependable representation of the physical ocean state, making it valuable for studying many ocean exploration tasks and enabling applications such as seasonal forecasts. Moreover, its high-quality data make it a valuable resource for regional purposes and provide essential physical parameters for areas such as marine biogeochemistry (Lellouche et al., 2021). We used geostrophic velocities at a depth of 0.5 m, which represents the uppermost layer in the GLORYS12V1 dataset, The spatial average of the data was taken at 1/12° latitude and longitude, with a temporal resolution of 1 day.

3. Results

3.1. Experiment 1. Direct Lagrangian Modeling of Marker Spread from the Fukushima Daiichi NPP

Experiment 1 was conducted using Lagrangian modeling, which consisted of the following: for 1 month after the disaster, from March 11 to April 9, 2011, 200,000 Lagrangian markers were launched daily at the segment (35.6° N, 141.0° E–38.2° N, 141.6° E) near FDNPP (the purple segment in Fig. 1), and their trajectories were tracked. The trajectory calculations were carried out 3 years ahead of time. The time and coordinates of reaching the eastern boundary of the East China Sea were recorded, which in the experiment was represented by the red segment between the islands of Taiwan and Kyushu, i.e., 25.1° N, 121.7° E–31.1° N, 130.6° E. In addition to this segment, a second (yellow) segment was selected with coordinates 24.5° N, 124.5° E–31.1° N, 130.6° E, running along the eastern periphery of the Kuroshio.

Figure 2 shows the dasymetric maps of the tracks of all markers launched and reaching the respective segments. The dasymetric maps of daily tracks of all markers represent maps that display the trajectories of markers simulating contamination as they move toward the selected segment. These maps visualize the paths taken by the markers in the water environment, depending on the circulation in the region and its temporal variability. The reason why the tracks for the yellow segment (Fig. 2b) extend significantly farther west than for the red segment (Fig. 2a), even though the red segment is located to the west of the yellow segment, is that the yellow segment is partially intersected by markers from the western side, meaning that the markers are initially advected southward from the segment and then carried eastward by the Kuroshio current.

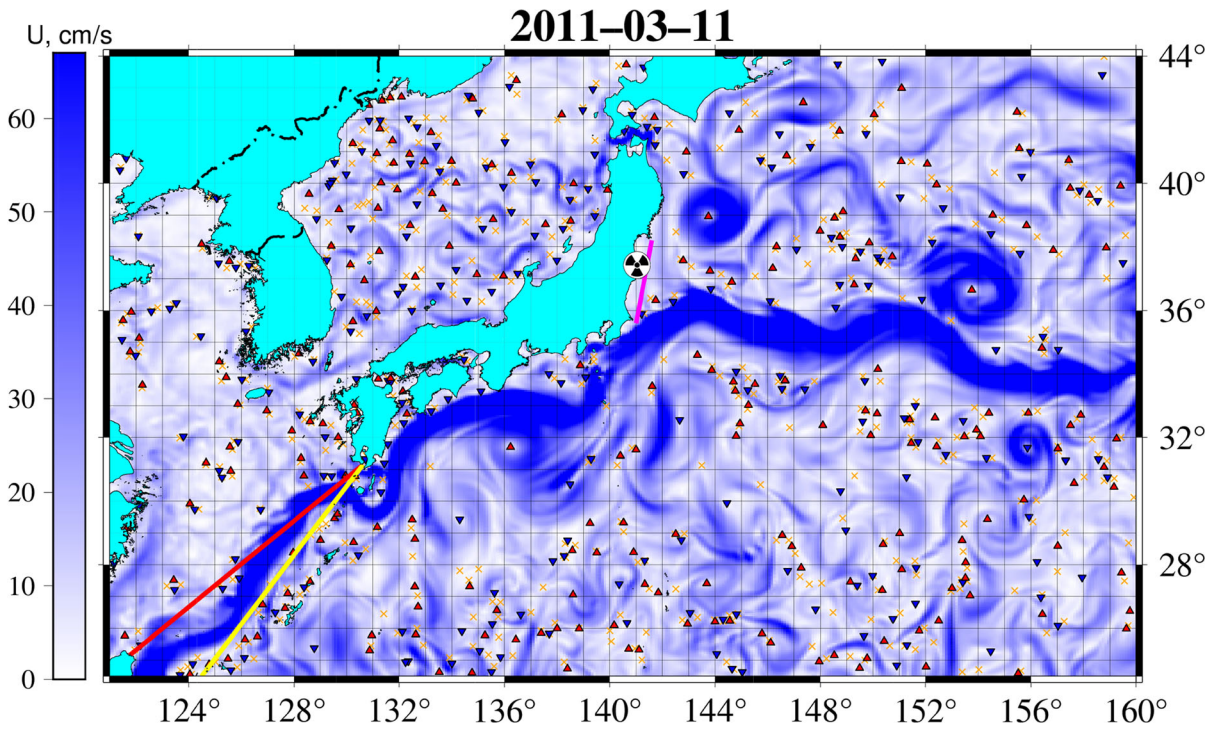

Fig. 1
Study area. The color shows the speed value (cm/s). The location of the FDNPP (coordinates 37° 25′ 12.0″ N, 141° 2′ 58.0″ E) is indicated by the radiation hazard symbol. The purple segment is the location of the daily launch of 200,000 Lagrangian markers (trajectories of simulated particles start here). The red (35.6° N, 141° E–38.3° N, 141.6° E) and yellow (24.5° N, 124.5° E–31.148264° N, 130.623008° E) segments are located in the eastern boundary of the East China Sea. The red triangles ▲ correspond to anticyclone centers, and the blue triangles ▼ indicate cyclones. The yellow crosses represent the hyperbolic points

Figure 3 shows the trajectories of the markers launched on the segment near the FDNPP (shown in purple on Fig. 1) on March 13, 2011, and reaching the red segment. Lagrangian modeling allows tracking the trajectories of only those markers that possess specific characteristics. Figure 3 presents the trajectories of markers that were launched on a specific date and reached the boundary of the East China Sea (the red segment). As we will see later (Fig. 6b), the choice of March 13, 2011, is not accidental: markers launched on this day reach the specified boundary in three batches (in May 2013, October–November 2013, and January–February 2014). Similar maps can be constructed for any date within the considered period from March 2011 to the end of March 2014, for which calculations were performed. Summary information on all trajectories is presented in the dasymetric maps in Fig. 2.

Figure 4 shows the distribution of markers by latitudes of crossing the corresponding segment. The calculations were performed for all markers, launched daily in the amount of 200,000 near FDNPP from March 11 to April 9, 2011. It is noteworthy that two touching zones are highlighted on the red segment (located along the western periphery of Kuroshio). From the perspective of potential westward penetration into the East China Sea, the most interesting latitude range is 25.5°–26° N. Two segments (red and yellow, see pls Fig. 1), are selected along the western and eastern peripheries of Kuroshio near the eastern boundary of the East China Sea. As seen in Fig. 4a, two peaks are observed: in the range 25.5°–26° N and 28.5°–30° N, and the markers cross the red segment strictly from east to west, as it is drawn from the northern shore of Taiwan Island to the southern shore of Kyushu Island. The crossing of this segment at its southern latitudes is associated

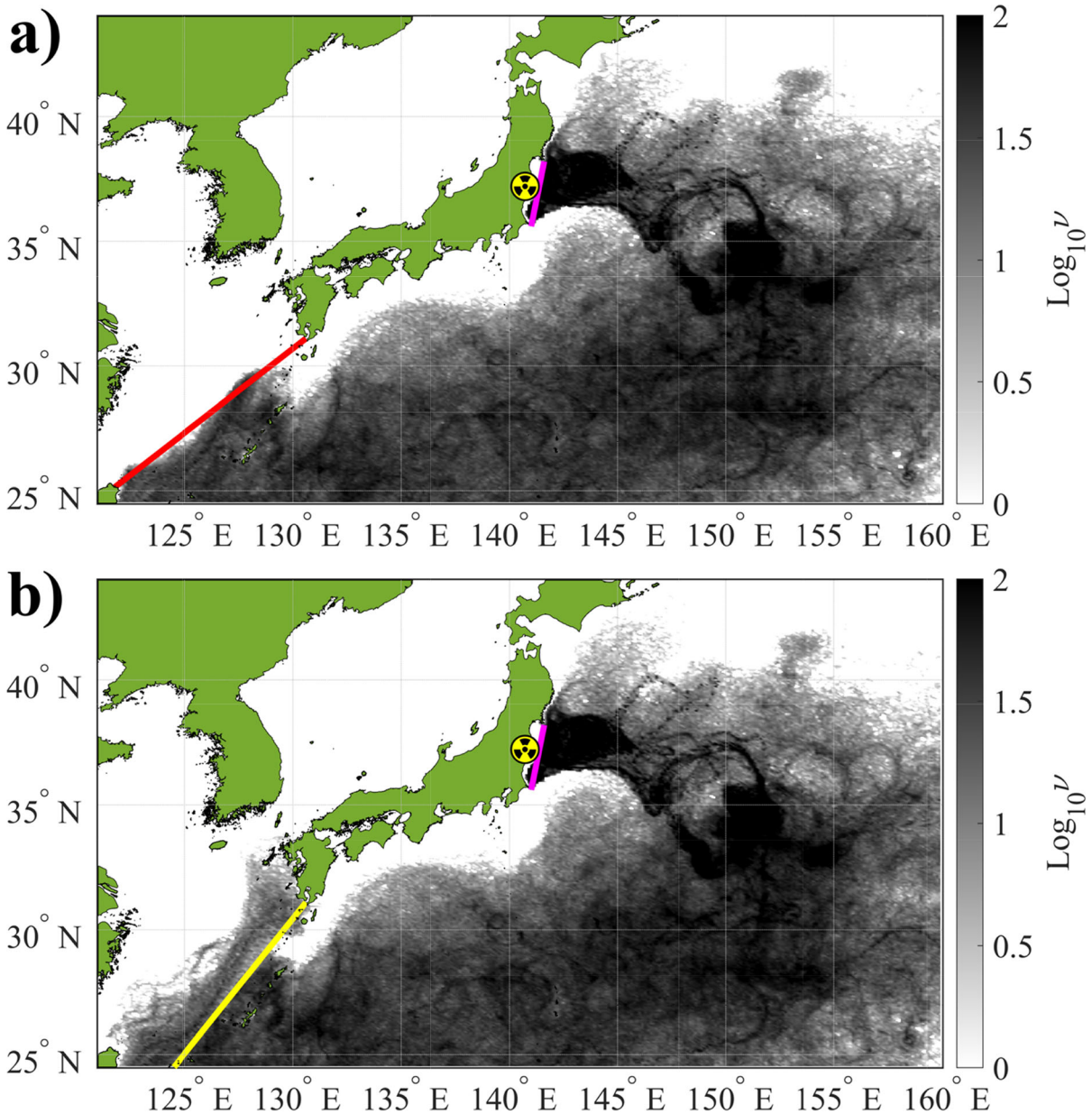

Fig. 2

Density (dasymetric) maps of daily trajectories of the markers released from the FDNPP launched from March 11 to April 9, 2011, near the Fukushima NPP (at the purple segment in Fig. 1), and reached the red (**a**) and yellow (**b**) segments. The velocity field in the calculations is based on GLORYS12V1 reanalysis data (surface layer). The scale presents $\nu = \log \varphi$, where φ is the density of daily tracks of the trajectories

either with the weakening of Kuroshio at this point or with vortex transport across the current. Additionally, it is linked to the intrusion of the Kuroshio Current into the East China Sea, a process extensively studied in the 1990s (Chuang & Liang, 1994; Hsueh et al., 1992; Nitani, 1972; Tang & Yang, 1993). The crossing of the yellow segment can occur with markers both from east to west and from west to east. It should be noted that all statistics were calculated up until the moment of the first crossing

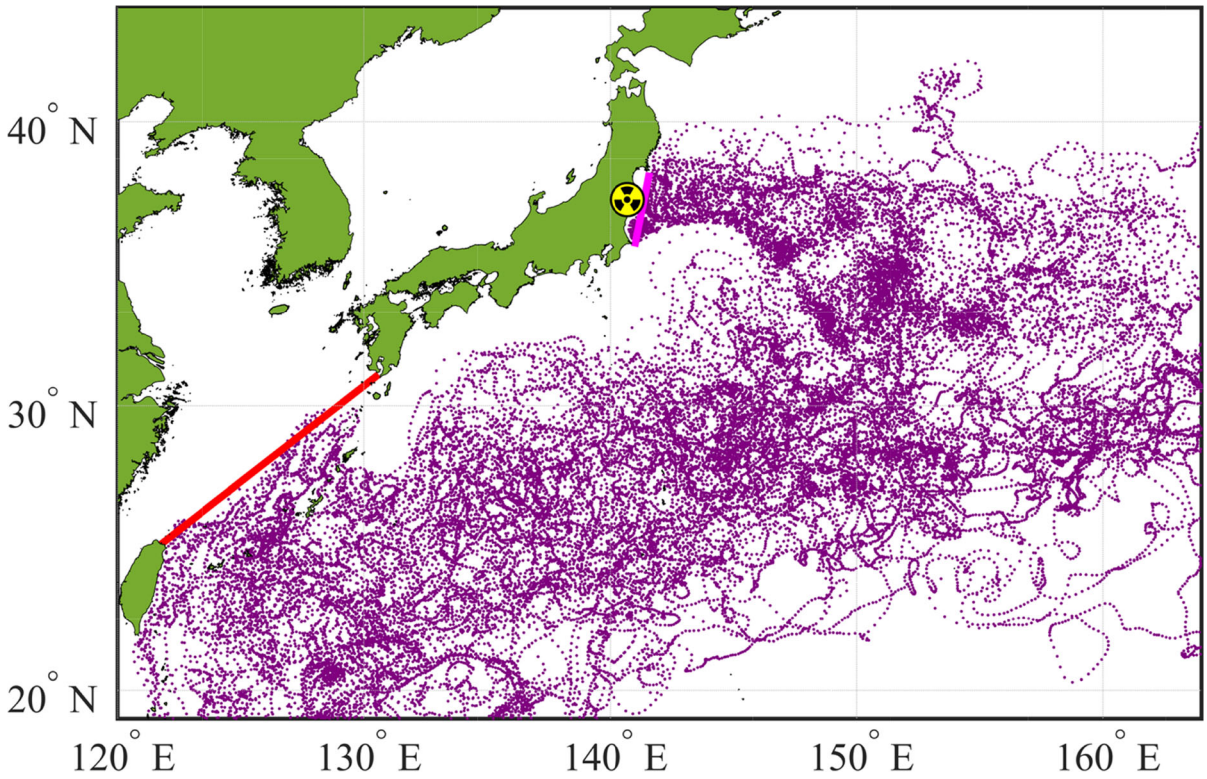

Fig. 3
Experiment 1 based on GLORYS12V1 data. Trajectories of markers launched from the FDNPP (on the purple segment) on March 13, 2011, and reached the red segment

of the markers' trajectories of the corresponding segment. Markers can cross the yellow segment from the west, initially bypassing it from the south, and then, being picked up by the Kuroshio current, crossing it in the latitude range from 24.5° to 28.5° N. The characteristic peak in the latitude range of 30°–31° N in Fig. 4b may be associated with the advection of markers to the yellow segment by vortices of different polarities, which move westward along the southern periphery of Kuroshio.

Figures 5, 6, 7, 8 show the distribution of markers based on various characteristics. Figure 5a shows the number of markers depending on the date of arrival. Recall that the markers were launched from the FDNPP in a quantity of 200,000 daily from March 11 to April 9, 2011 (see the purple segment in Fig. 1). It is evident that at the beginning of the experiment, the number of markers crossing the red segment is small, but it gradually increases and reaches a maximum in January 2014 (up to 80 markers per day), after which it begins to decrease. Figure 5b illustrates the distribution of the number of markers based on their travel time. This graph clearly shows the periodicity in the achievement of the red segment—the western boundary of Kuroshio, indicating the heterogeneous nature of marker transport over time. Distinct portions of potentially contaminated water are brought to the selected segment within specific time windows. It is worth noting that the time required for Lagrangian particles to reach the western boundary of the East China Sea ranges from 1.5 to 3 years, confirming the presence of long-term processes in the transport of water masses.

Figure 6a,c graphically shows the relationship between the latitude of the arrival of Lagrangian markers (y-axis) and the arrival date (x-axis) at the red segment. It is important to note that the markers arrive at the segment unevenly, both in time and space. The largest number of markers reaches the red segment at latitudes 26° N, 27° N, and especially in

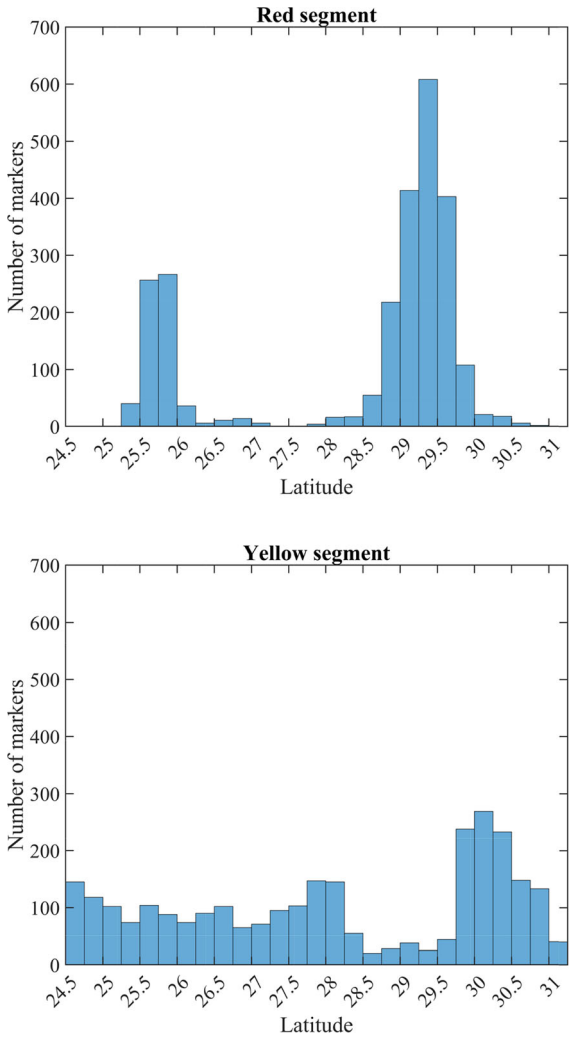

Fig. 4
Distribution of markers by latitudes of crossing the corresponding segment based on the number of all markers launched from the FDNPP (on the purple segment) from March 11 to April 9, 2011

the latitude range of 29°–30°N, which further confirms the periodicity of marker arrivals at the segment. This periodicity is also observed in Fig. 6b, d which shows the relationship between the launch date (y-axis) of Lagrangian markers from the FDNPP and the arrival time (x-axis) at the red segment. This figure highlights three groups of markers, confirming the presence of three peaks seen in Fig. 5b.

Figures 7 and 8 present similar results for markers transported from the FDNPP area to the yellow segment. The analysis shows that, as in the previous case, there is periodicity and uneven distribution of markers depending on the time of their movement. It is important to note that, as in Figs. 5b, 7b also shows three distinct peaks, reflecting the periodic arrival of potentially contaminated markers to both the western (red segment) and eastern (yellow segment) peripheries of the Kuroshio. The analysis of Figs. 5a and 7a reveals the significant role of seasonal cycles in shaping the transport pathways and temporal distribution of particles in this region. Generally, the trajectory areas of particle tracks exhibit strong seasonal variability and are also influenced by the East Asian Monsoon, which has a period of approximately half a year. This influence likely explains why the three peaks in Figs. 5b and 7b persist for nearly 150 days.

Let us consider Fig. 6, which consists of four parts. Figure 6c is a continuation of Fig. 6a, and d is a continuation of Fig. 6b. The release of Lagrangian particles in Experiment 1 took place on March 11, 2011, as shown on the *y*-axis (Fig. 6b). The *x*-axis in Fig. 6 represents the arrival dates of Lagrangian particles simulating contamination at the red segment. Figure 6b shows that the first particles reach the red segment as early as June 2012. Thus, it took the particles just over a year to travel from the location of the FDNPP to the red segment. Figure 6a shows the latitudes that record the latitude at which the corresponding Lagrangian particle crosses the red segment, which is located between 25.1° N and 31.1° N. In Fig. 6a, and especially in Fig. 6c, it is clearly visible that the particles cross the red segment at specific locations—primarily around 26° and particularly 30° north latitude. This localization of particles is associated with the circulation features in this region. By 2013, i.e., 2 years after the release of particles on March 11, 2011, the number of particles crossing the red segment significantly increased (Fig. 6c and d).

Figure 8 is similar to Fig. 6, but it pertains to the yellow segment. The yellow segment represents the boundary of the East China Sea, located much farther to the east. Since particles can reach the yellow segment from the south and also cross it from the opposite, i.e., western side, there is no strict localization of particles to specific latitudes, as seen in Fig. 6a and c. In Fig. 8a and c, the particles cross the yellow segment at almost all latitudes. However, it is

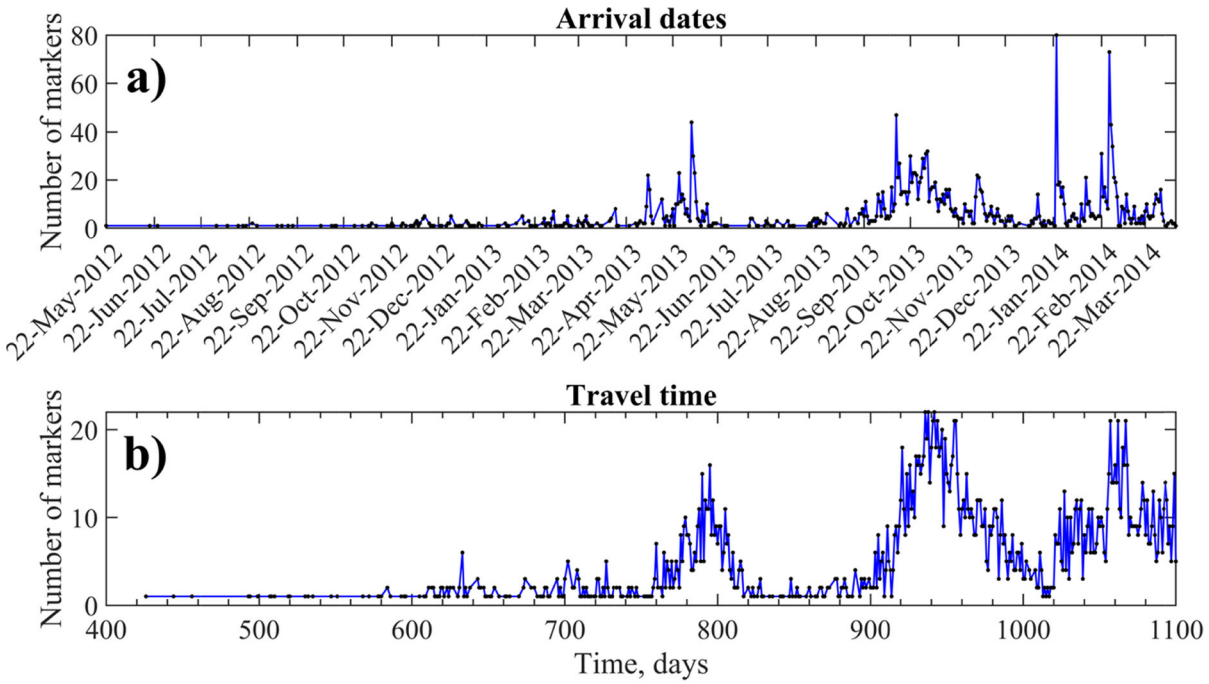

Fig. 5
(**a**) Distribution of the number of markers by arrival dates from the FDNPP to the red segment; (**b**) Distribution of the number of markers by advecting time from the FDNPP to the red segment

important to note that the time it takes for particles to travel from the location of the FDNPP to the yellow segment remains more 400 days from the release date of March 11, 2011.

3.2. Experiment 2. Modeling the Spread of a Marker Patch Simulating Pollution

The purpose of Experiment 2 is to study the spread of a marker patch (with a total of 200,000 markers) simulating pollution from the FDNPP in the ocean. As expected, the dynamics of the spread of this patch will depend on the characteristics of the ocean currents. As shown in Fig. 9, the majority of the markers in the patch first spread along the main current of the Kuroshio Extension. It is captured by the current and spreads eastward. Another portion of the markers "diffuses" in the mixing zone—between Oyashio and the northern periphery of the Kuroshio Extension. A third portion of the potentially polluted waters crosses the Kuroshio Extension to the south, being captured by cyclonic rings. It is important to note that the detachment of these rings occurs in three areas with longitudes: 145° E, 152° E, and 156° E (see Fig. 9). The formed rings are advected southwestward, and they may either break into several smaller ones or merge back with the main Kuroshio Extension current. The daughter vortices formed from the splitting may shift southward, deviating a significant distance from the main Kuroshio Extension current, which allows the potentially polluted waters captured by the cores of these vortices to be advected far southwest. We believe that these eddies are the primary transporters of particles simulating potentially polluted waters toward the yellow and red segments near the Kuroshio.

Figure 9 shows the trajectory length maps of the markers (calculated for 30 days of backward time)—S-maps and velocity fields from GLORYS12V1 (0.5-m horizon), along with fragments of the marker patch (crimson) evolution, launched on March 13, 2011, based on GLORYS12V1 data. The patch and the visualization dates were selected based on the analysis of Figs. 5, 6, 7, 8.

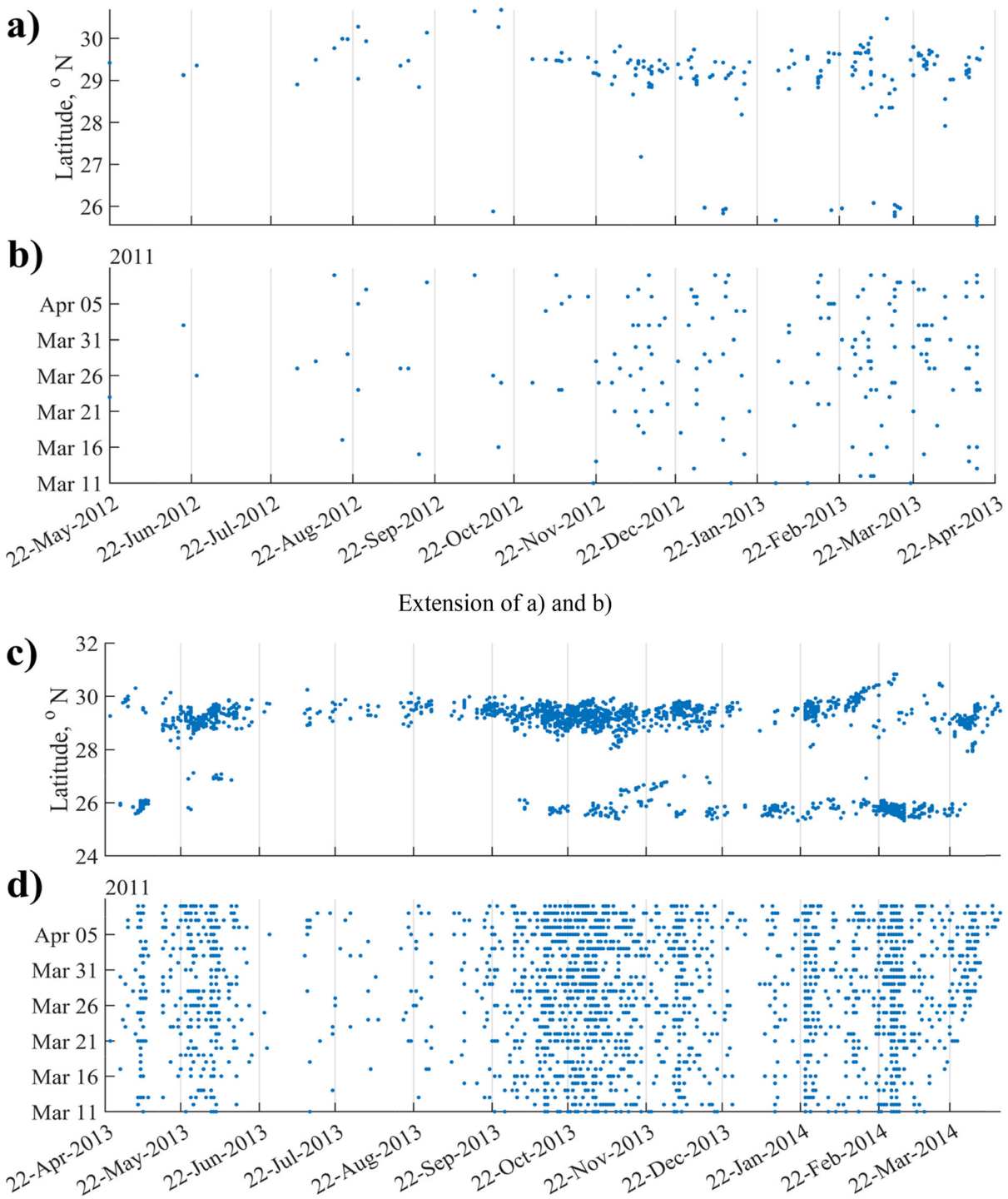

In Fig. 9, it can be seen that eddies with high marker concentrations periodically detach from the main Kuroshio current, along which the potential pollution patch spreads. The analysis showed that these vortical structures are cyclones. These cyclones, filled with markers simulating polluted waters, repeatedly detach from the main current and reconnect with it, demonstrating behavior similar to that of

◀Fig. 6
From May 22, 2012, to April 22, 2013: (**a**) Dependence of the latitude (*y*-axis) of Lagrangian marker arrivals at the red segment on the arrival date (*x*-axis); (**b**) Dependence of the launch date of Lagrangian markers from the FDNPP (*y*-axis) on the arrival time (*x*-axis) at the red segment; From April 22, 2013 to April 11, 2014: (**c**) Dependence of the latitude (*y*-axis) of Lagrangian marker arrivals at the red segment on the arrival date (*x*-axis); (**d**) Dependence of the launch date of Lagrangian markers from the FDNPP (*y*-axis) on the arrival time (*x*-axis) at the red segment

a ping-pong ball in motion. This process is an example of cross-jet transport, where water or pollution particles cross the main current, being captured by vortical structures.

Cross-jet transport plays an important role in the transfer of pollutants and other passive tracers in the ocean, ensuring their effective mixing and dispersion beyond the main flow. In the context of Kuroshio, this process allows a significant portion of the markers to cross the core of the current, facilitating their further movement southward. Such processes enhance the horizontal exchange of substances in oceanic systems and form complex patterns of spatial distribution of passive tracers. However, eventually, after detaching from the main current, these cyclones begin to shift southward, where they gradually dissipate.

As the eddies dissipate, the markers previously concentrated in cyclonic structures mix with the surrounding water mass. Some of them, being captured by other vortex formations, continue to move southwestward. This transport process, which involves repeated cycles of capture and transport by individual eddies, causes the markers to reach the eastern boundary of the East China Sea, demonstrating the complex, multi-component nature of their distribution.

4. Discussion and Conclusions

After the FDNPP accident in 2011, potentially contaminated waters could have been transported to the eastern boundary of the East China Sea. The primary mechanism for this transport is the influence of the Kuroshio Current, which captures the

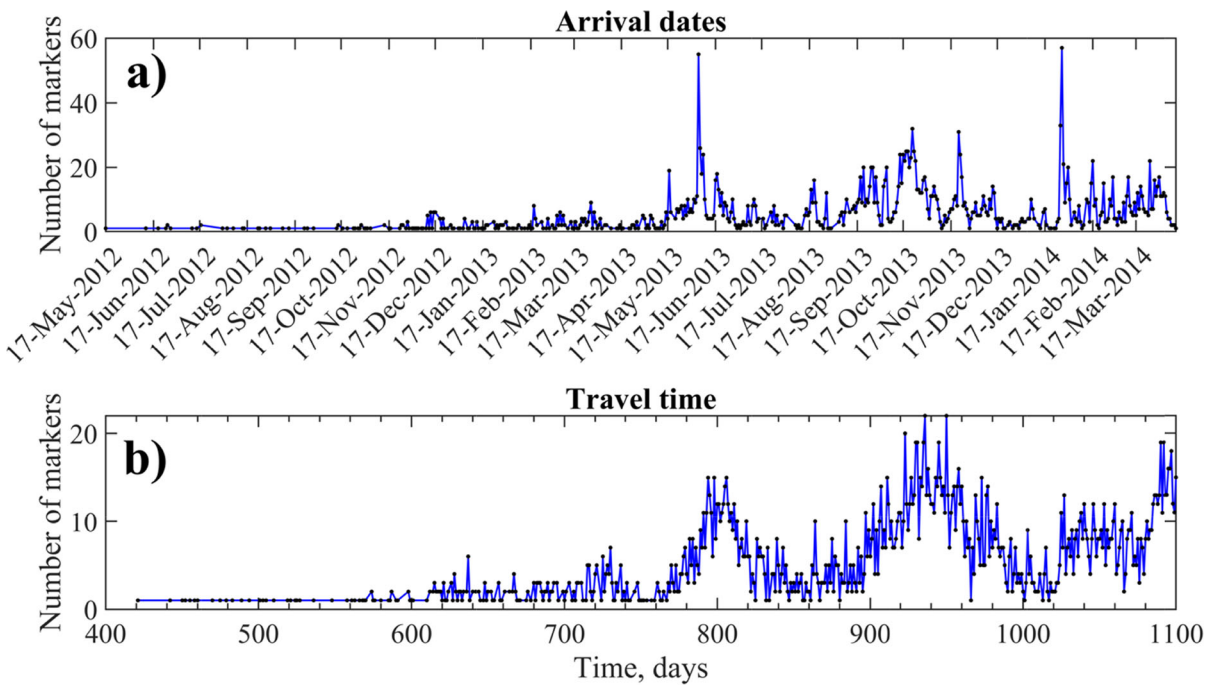

Fig. 7
The same as in Fig. 5, for the yellow segment

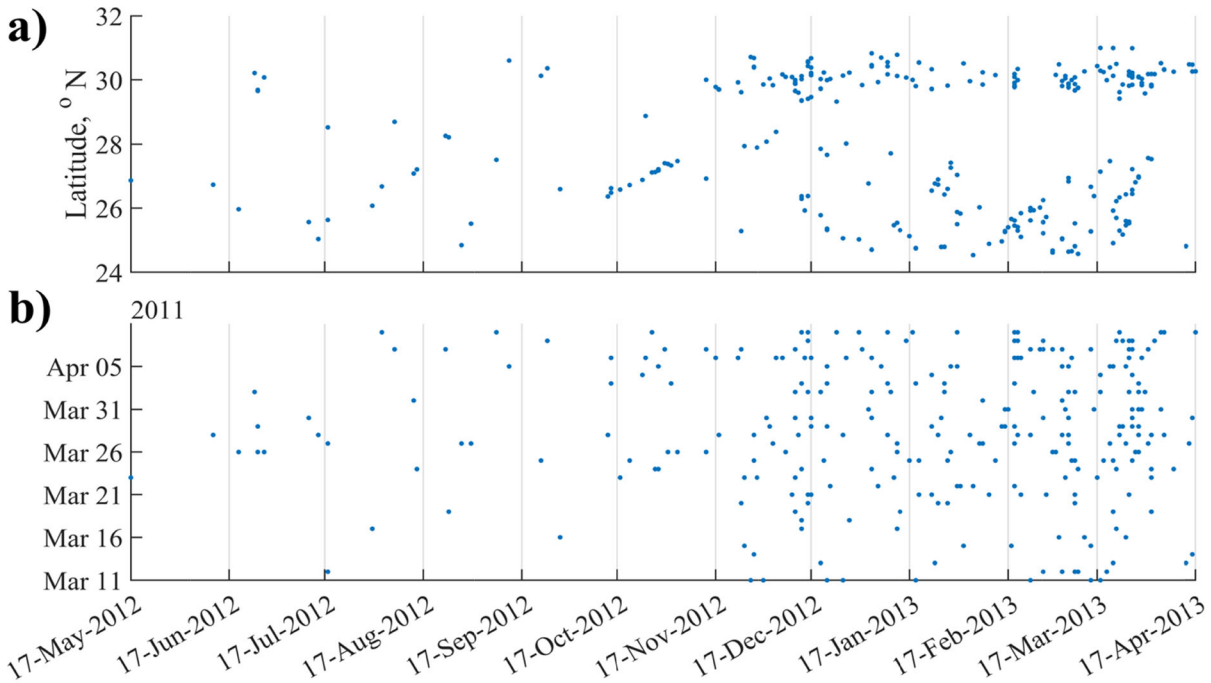

Extension of a) and b)

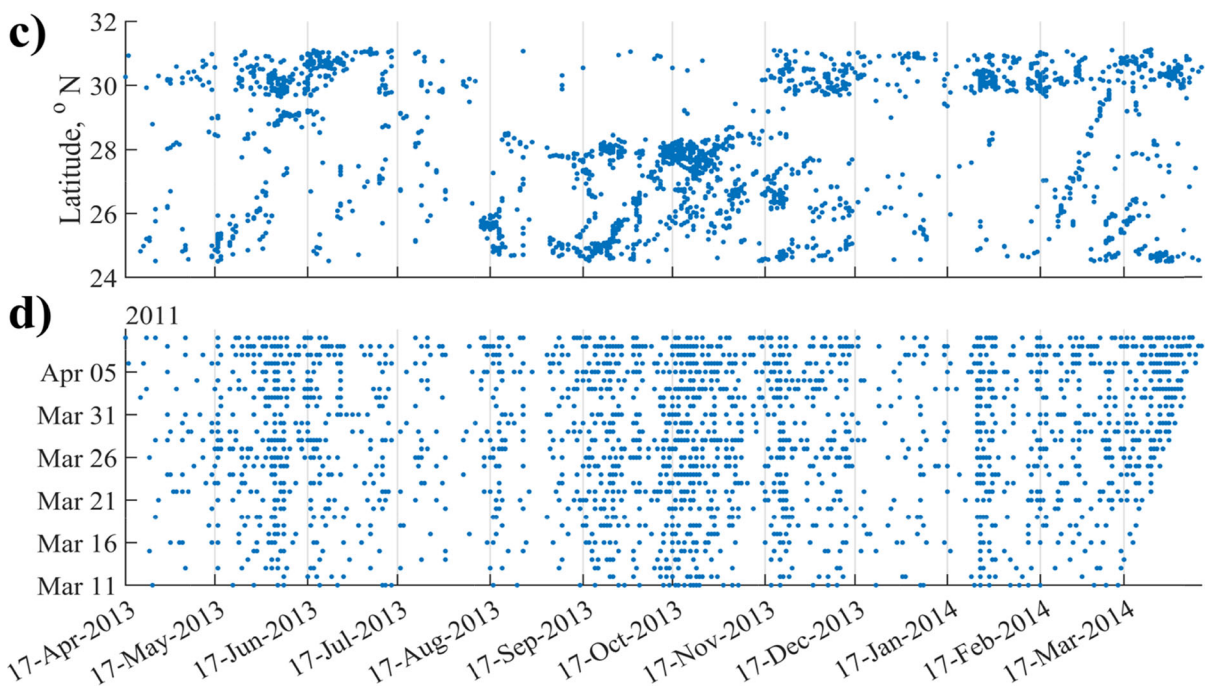

contaminated waters, forming cyclonic rings. These rings, in turn, detach from the main current and transport the contaminated waters southwestward. The dissipation of the cyclonic eddies contributes to the further movement of pollution toward the eastern periphery of the Kuroshio.

Using Lagrangian methods, Kim et al. (2024), Lee et al. (2023), and particularly Cedarholm et al. (2019)

◀Fig. 8
From May 17, 2012, to April 17, 2013: (**a**) Dependence of the latitude (*y*-axis) of Lagrangian marker arrivals at the yellow segment on the arrival date (*x*-axis); (**b**) Dependence of the launch date of Lagrangian markers from the FDNPP (*y*-axis) on the arrival time (*x*-axis) at the yellow segment; From April 17, 2013 to April 12, 2014: (**c**) Dependence of the latitude (*y*-axis) of Lagrangian marker arrivals at the yellow segment on the arrival date (*x*-axis); (**d**) Dependence of the launch date of Lagrangian markers from the FDNPP (*y*-axis) on the arrival time (*x*-axis) at the yellow segment

demonstrate the fundamental possibility of transporting particles simulating radionuclide contamination to the NPSTMW region—the North Pacific Subtropical Mode Water. Kim et al. (2024) consider virtual particle trajectories calculated over a 5-year period, from January 1, 1994, to December 31, 1998. Lee et al. (2023) analyzed a forward-tracking simulation conducted on the 25.2σ isopycnal surface, which is the core layer of the NPSTMW. Using a 3-dimensional hydrodynamic model, they reported that a radioactive tracer originating from the Fukushima Daiichi Nuclear Power Plant (FDNPP) took approximately 8–9 years to reach the Taiwan and Philippine islands, following a clockwise trajectory; however, there may have been limited southward movement that dissipated rapidly. Cedarholm et al. (2019), based on a Lagrangian approach, constructed trajectories of virtual particles propagating into the NPSTMW from the Kuroshio Extension (KE).

Measurements of the distribution of plutonium in the sediments (Wang & Liu, 2020) and concentration of radioactive cesium in the seawater of the East China Sea have shown that some amount of it is from the FDNPP accident (Aoyama et al., 2017; Kaeriyama, 2015, 2017; Inoue et al., 2018). There are several ways of transporting nuclear pollution to the semi-closed seas.

Massive energetic cyclonic and anticyclonic eddies with a diameter of tens to hundreds of kilometers are generated from the Kuroshio meanders and the collision of the warmer Kuroshio and colder Oyashio. These eddies and the southern recirculation, together with turbulent diffusion can transport the radionuclides toward the East China Sea. Many of these eddies are highly nonlinear and capable of advecting the radionuclides long distances with high concentration and low dissipation. Eddies near the Kuroshio Extension also significantly increase subduction of the radionuclides into the mode water, a thick layer of water with homogeneous properties in the subsurface ocean; through recirculation, the radionuclides can be quickly transported toward the East China Sea. The numerical simulation shows that the radionuclides reach the East China Sea in about 1 year. The Kuroshio branch in the East China Sea further transports the radionuclides northeastward, and exchanges significantly with the East China Sea shelf current. As a result, the radionuclides appear in the Yellow Sea and Japan Sea further north (Boening, 2012; Chen et al., 2021). The radionuclides come mainly from the Taiwan Strait and the waterway east of Taiwan (Rong & Liang, 2018).

Model results are proven by the statistics of surface drifter data. Those statistic is show three types of transport paths for nuclear pollutants at the surface: (1) most pollutant particles move eastward and are carried by the Kuroshio and Kuroshio-extension currents and reach the east side of the North Pacific after about 3.2–3.9 years; (2) some particles travel with the subtropical circulation branch and reach the east coast of China after about 1.6 years according to one drifter trajectory and about 3.6 years according to particulate trajectories; (3) a little of them travel with local, small scale circulations and reach the east coast of China after about 1.3–1.8 years (Fu et al., 2014; Han et al., 2013).

Thus, there are several studies demonstrating the propagation of potentially contaminated water to the border of the East China Sea. Our study confirms these results. Nevertheless, we advance our analysis by providing quantitative estimates of the arrival of Lagrangian particles originating from FDNPP to the boundary of the East China Sea. Furthermore, we establish that the dominant mechanism governing particle transport to this region is vortex-driven advection, which results in the non-uniform, episodic influx of particles in discrete batches. These batches are advected southward through the meandering pathways of vortical structures. This phenomenon is depicted in Fig. 4 and is particularly evident in Figs. 5 and 7.

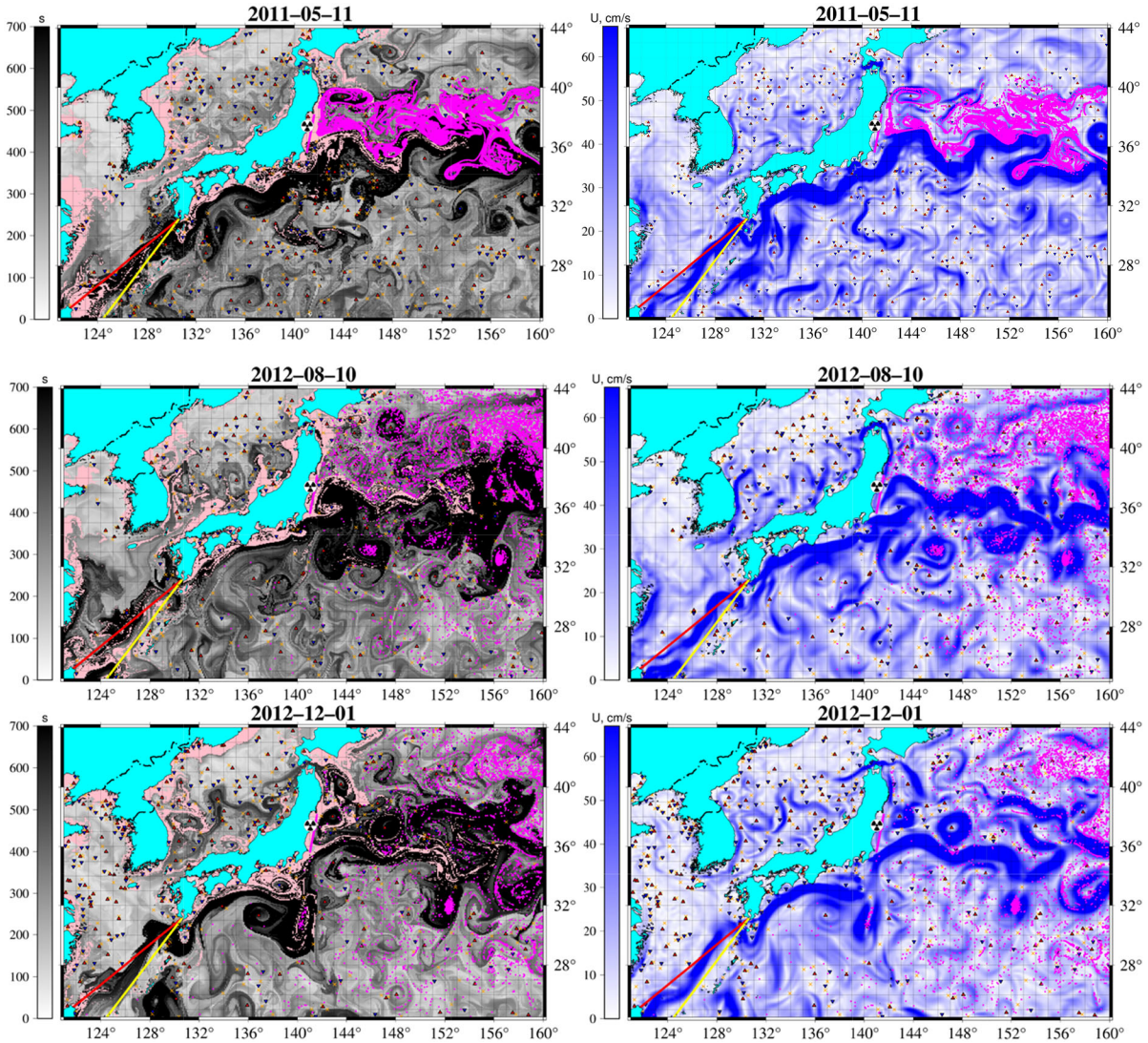

Fig. 9

Experiment 2 based on GLORYS12V1 data. Examples of S maps (left) and velocity fields (cm/s, right) for selected dates. The color scale of S corresponds to the distance (in kilometers) traveled by the markers over 30 days. Evolution of the marker patch consisting of 200,000 markers launched on March 13, 2011, from the FDNPP. The marker patch is shown in magenta. Red triangles ▲ denote anticyclone centers, and blue triangles ▼ indicate cyclones. The yellow crosses represent the hyperbolic points

Figures 6 and 8 are of great importance, as they show that the time required to reach the boundary of the East China Sea is not 8–9 years, but significantly shorter. As shown in Sect. 3.1, the first particles reach the East China Sea boundary in over a year. We performed a precise count of particles reaching the red or yellow segments and calculated the time it takes for particles to cross the NPSTMW region and reach the boundary of the East China Sea. This period is considerably shorter than the 8–9 years reported in the study by Lee et al. (2023).

The transport of contaminated waters can also occur via cross-jet advection when eddies formed due to the weakening of the Kuroshio Current near Taiwan drive the contamination westward.

During the southward transportation of contaminated water to the vicinity of Taiwan Island, it was influenced by the East Asian monsoons, resulting in a

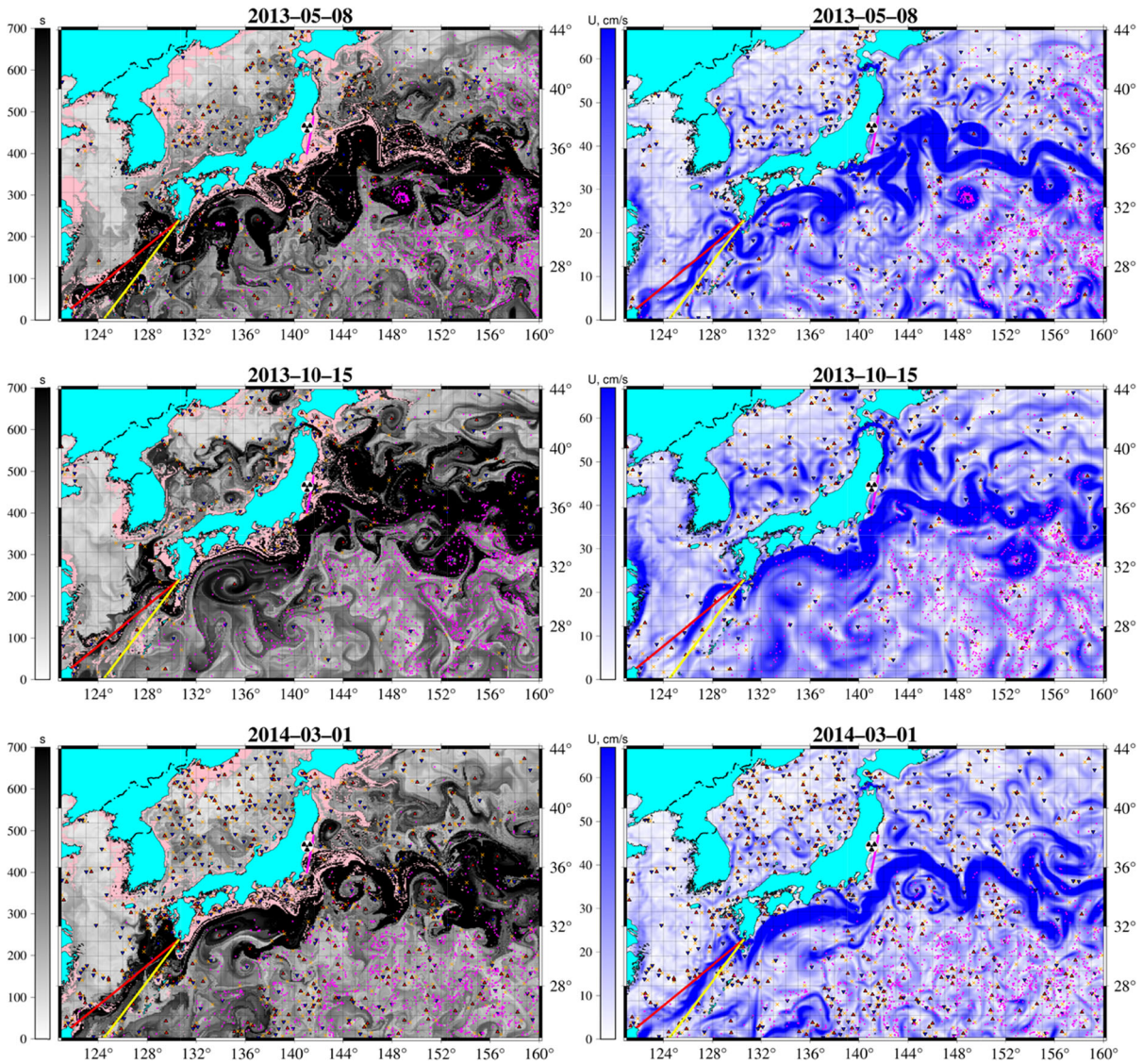

Fig. 9
continued

6-month recurrence cycle. Due to the sustained transport of monsoon and eddies, the flux of contaminated water has long-term sustainability and can cause stable accumulation in the region. The 6-month cyclicity is evident in Figs. 5 and 7.

Thus, for the transport of markers simulating pollution, a combination of three factors is necessary: (1) cross-jet transport of the Kuroshio Extension and the formation of corresponding cyclonic rings containing markers in their core, (2) advection of the formed rings or their daughter eddies southwestward, (3) a specific Kuroshio regime that allows the transport of markers from east to west across the Kuroshio Current due to its weakening.

Answering the question posed in the title of this study—"Can contaminated waters from the FDNPP penetrate the East China Sea?"—we affirmatively conclude that such penetration is indeed possible. Moreover, it will take the particles just over a year to spread from the FDNPP to the East China Sea.

The question of the permeability of the Kuroshio near the northern coast of Taiwan in the fall of 2013, as well as during the dates of marker arrival (see Figs. 5, 6 and 7, 8), remains unresolved. A detailed description of the behavior of the Kuroshio during these dates is required.

Author Contributions BTV and BMV wrote the main manuscript text; BTV is responsible for literature review and first draft writing; BMV is responsible for particle tracking modeling; BMV, BTV, and UMYu are responsible for conceptualization; LMA, UMYu, FPA, BMV, DT, XY, and SY andresponsible for data analysis; BMV, DAA, and LMA are responsible for preparing the figures; All authors reviewed the manuscript.

Funding

The research was carried out with the support of St. Petersburg University, grant No. 116442164. The work of M.B. and A.U. on the Lagrangian analysis of passive marker advection is supported with the help of a high-performance computing cluster at the Pacific Oceanological Institute (State Task No. 124022100072-5), the program 'Fundamental principles of adaptation strategies for the development of the Russian Far East in the context of global climate change' at POI FEBRAS, and by the PI Project of the Southern Marine Science and Engineering Guangdong Laboratory (Guangzhou) (GML2021GD0810), and the Guangdong Special Support Program of the Southern Marine Science and Engineering Guangdong Laboratory (Guangzhou) (2019BT02H594).

Data Availability

We use current velocities on the surface obtained from the global high-resolution ocean reanalysis GLORYS12V1 (Global Ocean Physics Reanalysis) with a spatial resolution of 1/12° from Copernicus Marine Service (https://marine.copernicus.eu/) available at https://doi.org/10.48670/moi-00021. Product user manual for sea level SLA products. CMEMS-SL-PUM-008-032-062, Copernicus Marine Service, 39 pp., http://marine.copernicus.eu/documents/PUM/CMEMSSL-PUM-008-032-062.pdf.

Declarations

Conflict of interest The authors declare that they have no conflict of interest.

Publisher's Note Springer Nature remains neutral with regard to jurisdictional claims in published maps and institutional affiliations.

References

Aoki, S., Imawaki, S., & Ichikawa, K. (1995). Baroclinic disturbances propagating westward in the Kuroshio Extension region as seen by a satellite altimeter and radiometers. *Journal of Geophysical Research, 100*(C1), 839. https://doi.org/10.1029/94jc02255

Aoyama, M., Hamajima, Y., Inomata, Y., & Oka, E. (2017). Recirculation of FNPP1-derived radiocaesium observed in winter 2015/2016 in coastal regions of Japan. *Applied Radiation and Isotopes, 126*, 83–87. https://doi.org/10.1016/j.apradiso.2016.12.003

Belonenko, T. V., Budyansky, M. V., Akhtyamova, A. F., & Udalov, A. A. (2024). Investigation of the Benguela upwelling eddies using Lagrangian modeling methods. *Ocean Dynamics, 74*(5), 373–390. https://doi.org/10.1007/s10236-024-01609-8

Belonenko, T. V., Koldunov, V. V., Staritsyn, D. K., Fuchs, V. R., & Shilov, I. O. (2009). *Variability of sea level in the Northwestern Pacific* (p. 309). St Petersburg: SMIO-PRESS Publishing House. ISBN 978-5-7704-0220-9.

Belonenko, T. V., & Kubryakov, A. A. (2014). Temporal variability of the phase velocity of Rossby waves in the North Pacific. *Sovremennye Problemy Distantsionnogo Zondirovaniya Zemli Iz Kosmosa [modern Problems of Remote Sensing of the Earth from Space], 11*(3), 9–18.

Bernstein, R. L., & White, W. B. (1981). Stationary and traveling mesoscale perturbations in the Kuroshio Extension current. *Journal of Physical Oceanography, 11*(5), 692–704. https://doi.org/10.1175/1520-0485(1981)011%3c0692:satmpi%3e2.0.co;2

Boening, C. (2012). Model simulations on the long-term dispersal of 137 Cs released into the Pacific Ocean off Fukushima. *Environmental Research Letters, 7*(3), 034004. https://doi.org/10.1088/1748-9326/7/3/034004

Budyansky, M. V., Belonenko, T. V., Lebedeva, M. A., & Udalov, A. A. (2024a). Surface transport of technical waters from Fukushima NPP to the South Kuril Fishing Zone. *Russian Journal of Earth Sciences*. https://doi.org/10.2205/2024es000934

Budyansky, M. V., Goryachev, V. A., Kaplunenko, D. D., Lobanov, V. B., Prants, S. V., Sergeev, A. F., Shlyk, N. V., &

Uleysky, M. Y. (2015). Role of mesoscale eddies in transport of Fukushima-derived cesium isotopes in the ocean. *Deep Sea Research Part i: Oceanographic Research Papers, 96*, 15–27. https://doi.org/10.1016/j.dsr.2014.09.007

Budyansky, M. V., Udalov, A. A., Lebedeva, M. A., & Belonenko, T. V. (2024b). Assessment of pollution of the waters in the South Kuril fishing zone of Russia by radioactive waters from the Fukushima-1 NPP based on Lagrangian modeling. *Doklady Earth Sciences, 515*(Part 1), 458–467. https://doi.org/10.1134/S1028334X2360305X

Burkov, V. A. (1992). Structure and variability of wave and vortex fields in the Kuroshio and Oyashio interaction zone, 24–81. In *The Megalopoligon experiment* (p. 415). Nauka **(in Russ.)**.

Cedarholm, E. R., Rypina, I. I., Macdonald, A. M., & Yoshida, S. (2019). Investigating subsurface pathways of Fukushima cesium in the northwest Pacific. *Geophysical Research Letters, 46*, 6821–6829. https://doi.org/10.1029/2019GL082500

Chen, G., Wang, Q., & Chu, X. (2021). Accelerated spread of Fukushima's waste water by ocean circulation. *The Innovation, 2*(2), 100119. https://doi.org/10.1016/j.xinn.2021.100119

Chen, R., McClean, J. L., Gille, S. T., & Griesel, A. (2014). Isopycnal eddy diffusivities and critical layers in the kuroshio extension from an eddying ocean model. *Journal of Physical Oceanography, 44*(8), 2191–2211. https://doi.org/10.1175/JPO-D-13-0258.1

Chuang, W. S., & Liang, W. D. (1994). Seasonal variability of intrusion of the Kuroshio water across the continental shelf northeast of Taiwan. *Journal of Oceanography, 50*(5), 531–542.

Delman, A. S., McClean, J. L., Sprintall, J., Talley, L. D., Yulaeva, E., & Jayne, S. R. (2015). Effects of Eddy vorticity forcing on the mean state of the Kuroshio extension. *Journal of Physical Oceanography, 45*(5), 1356–1375. https://doi.org/10.1175/jpo-d-13-0259.1

Ferrari, R., & Nikurashin, M. (2010). Suppression of Eddy diffusivity across jets in the Southern Ocean. *Journal of Physical Oceanography, 40*, 1501–1519. https://doi.org/10.1175/2010JPO4278.1

Fu, H., Li, W., Zhang, X., et al. (2014). A study of transport and impact strength of Fukushima nuclear pollutants in the north pacific surface. *Journal of Ocean University of China, 13*, 183–190. https://doi.org/10.1007/s11802-014-1942-9

Han, G., Li, W., Fu, H., et al. (2013). An ensemble estimation of impact times and strength of Fukushima nuclear pollution to the east coast of China and the west coast of America. *Science China Earth Sciences, 56*, 1447–2145. https://doi.org/10.1007/s11430-012-4520-2

Hiroaki, S. (2019). The Kuroshio: Its recognition, scientific activities and emerging issues. In *Kuroshio current—Physical, biogeochemical, and ecosystem dynamics* (pp. 3–12). Verlag American Geophysical Union.

Hsueh, Y., Wang, J., & Chern, C. S. (1992). The intrusion of the Kuroshio across the continental shelf northeast of Taiwan. *Journal of Geophysical Research, 97*(C9), 14323–14330.

Inoue, M., Shirotani, Y., Nagao, S., Aramaki, T., Kim, Y. I., & Hayakawa, K. (2018). Spatial variations of 226Ra, 228Ra, 134Cs, and 137Cs concentrations in western and southern waters off the Korean Peninsula in July 2014. *Journal of Environmental Radioactivity, 182*, 151–156. https://doi.org/10.1016/j.jenvrad.2017.11.020

Kaeriyama, H. (2015). 134Cs and 137Cs in the seawater around Japan and in the North Pacific. In: K. Nakata, & H. Sugisaki (Eds.), *Impacts of the Fukushima nuclear accident on fish and fishing grounds*. Springer. https://doi.org/10.1007/978-4-431-55537-7_2

Kaeriyama, H. (2017). Oceanic dispersion of Fukushima-derived radioactive cesium: A review. *Fisheries Oceanography, 26*(2), 99–113. https://doi.org/10.1111/fog.12177

Kamenkovich, V. M., Koshlyakov, M. N., & Monin, A. S. (1986). *Synoptic Eddies in the Ocean* (p. 444). Springer.

Kawai, H. (1980). Rings south of the Kuroshio and their possible roles in transport of the intermediate salinity minimum and in formation of the skipjack and albacore fishing grounds. In *The Kuroshio IV: Proc. 4th CSK Symp., Tokyo, 1979* (pp. 250–273). Saikon Publ. Co.

Kim, S.-Y., Lee, H. J., Jung, K. T., Kim, H., & Kim, K. O. (2024). A study on the pathways and their interannual variability of the Fukushima derived tracers in the northwestern Pacific. *Frontiers in Marine Science, 11*, 1358032. https://doi.org/10.3389/fmars.2024.1358032

Kitano, K. (1975). Some properties of the warm Eddies generated in the confluence zone of the Kuroshio and Oyashio currents. *Journal of Physical Oceanography, 5*(2), 245–252. https://doi.org/10.1175/1520-0485(1975)005%3c0245:SPOTWE%3e2.0.CO;2

Kitano, K. (1980). Some aspects of the historical development on the studies of the Kuroshio and the Oyashio. In M. Sears, & D. Merriman (Eds.), Oceanography: The past. Springer. https://doi.org/10.1007/978-1-4613-8090-0_26

Koshlyakov, M. N., & Monin, A. S. (1978). Synoptic Eddies in the Ocean. *Annual Review of Earth and Planetary Sciences, 6*, 495–523.

Lee, S.-T., Jung, J., Kim, G., Tak, Y.-J., & Cho, Y.-K. (2023). Subsurface dispersion path and travel time of radiocesium from Fukushima by Mode Water. *Frontiers in Marine Science, 10*, 1104786. https://doi.org/10.3389/fmars.2023.1104786

Lellouche, J.-M., Greiner, E., Romain, B.-B., et al. (2021). The copernicus global 1/12° oceanic and sea ice GLORYS12 reanalysis. *Frontiers in Earth Science, 9*, 698876. https://doi.org/10.3389/feart.2021.698876

Li, S., Wang, B., Deng, Z., et al. (2024). Data quality control method of a new drifting observation technology named drifting air-sea interface buoy. *Journal of Ocean University of China, 23*(1), 11–22. https://doi.org/10.1007/s11802-024-5426-2

Nitani, H. (1972). Beginning of the Kuroshio. In H. Stommel & K. Yoshida (Eds.), *The Kuroshio—Its physical aspects* (pp. 129–163). University of Tokyo Press.

Prants, S. V. (2014). Chaotic Lagrangian transport and mixing in the ocean. *The European Physical Journal Special Topics, 223*(13), 2723–2743. https://doi.org/10.1140/epjst/e2014-02288-5

Prants, S. V., Budyansky, M. V., & Uleysky, M. Y. (2014). Lagrangian study of surface transport in the Kuroshio Extension area based on simulation of propagation of Fukushima-derived radionuclides. *Nonlinear Processes in Geophysics, 21*(1), 279–289. https://doi.org/10.5194/npg-21-279-2014

Prants, S., Budyansky, M., & Uleysky, M. (2017a). Statistical analysis of Lagrangian transport of subtropical waters in the Japan Sea based on AVISO altimetry data. *Nonlinear Processes in Geophysics, 24*(1), 89–99. https://doi.org/10.5194/npg-24-89-2017

Prants, S. V., Budyansky, M. V., & Uleysky, M. Y. (2017b). Lagrangian simulation and tracking of the mesoscale eddies

contaminated by Fukushima-derived radionuclides. *Ocean Science, 13*, 453–463. https://doi.org/10.5194/os-13-453-2017

Prants, S. V., Uleysky, MYu., & Budyansky, M. V. (2017c). *Lagrangian oceanography: Large-scale transport and mixing in the ocean. Physics of earth and space environments*. Springer.

Rong, Y., & Liang, X. S. (2018). A study of the impact of the Fukushima Nuclear Leak on East China Coastal Regions. *Atmosphere-Ocean, 56*(4), 254–267. https://doi.org/10.1080/07055900.2017.1421139

Takeyoshi, N., Kazuyuki, O., & Hiroshi, N. (2019). The research advancements and historical episodes brought by the Kuroshio flowing across generations. In *Kuroshio current—Physical, biogeochemical, and ecosystem dynamics* (pp. 13–22). Verlag American Geophysical Union.

Tang, T. Y., & Yang, Y. J. (1993). Low frequency current variability on the shelf break northeast of Taiwan. *Journal of Oceanography, 49*(2), 193–210.

Tomosada, A. (1986). Generation and decay of Kuroshio warm-core rings. *Deep Sea Research Part a. Oceanographic Research Papers, 33*(11–12), 1475–1486. https://doi.org/10.1016/0198-0149(86)90063-4

Udalov, A., Budyansky, M., & Prants, S. (2023). A census and properties of mesoscale Kuril eddies in the altimetry era. *Deep-Sea Research I, 200*, 104129. https://doi.org/10.1016/j.dsr.2023.104129

Ueno, H., Bracco, A., Barth, J. A., et al. (2023). Review of oceanic mesoscale processes in the North Pacific: Physical and biogeochemical impacts. *Progress in Oceanography, 212*, 102955. https://doi.org/10.1016/j.pocean.2022.102955

Wang, R., & Liu, Z. (2020). Distribution and source of Pu in the sediments of the seas and estuaries of China—A review. *Anthropocene Coasts, 3*, 53–75. https://doi.org/10.1139/anc-2019-0017

(Received December 11, 2024, revised February 18, 2025, accepted February 22, 2025)